9

Hydrodynamic properties of proteins

STEPHEN E. HARDING

1. Renaissance of hydrodynamic techniques

Since the first edition of this book, there has been something of a renaissance of hydrodynamic methods for the determination of the mass, quaternary structure, gross conformation, and interaction properties of proteins and other macromolecules in solution. By 'hydrodynamic' (Greek for 'water-movement') techniques, we mean any technique involving motion of a macromolecule with or relative to the aqueous solvent in which it is dissolved or suspended. This therefore includes not only gel filtration, viscometry, sedimentation (velocity and equilibrium), and rotational diffusion probes (fluorescence anisotropy depolarization and electric–optical methods), but also 'classical' and 'dynamic' light scattering, which both derive from the relative motions of the macromolecular solute in relation to the solvent. This definition also includes electrophoretic methods (considered in Chapter 8 and not covered here), which are powerful tools for separation, purification, and identification of proteins, but also, with 'SDS' methodology, provide an estimate of polypeptide molecular weight (see Chapter 1). The present chapter therefore considers the hydrodynamic determination of 'molar mass' or molecular weight and quaternary structure (subunit composition and arrangement, self-association phenomena, and polydispersity). It will also consider the measurement of protein conformation in dilute solution with particular reference to the use of the analytical ultracentrifuge, a technique although of considerable antiquity (70th birthday in 1993) that has been the centre of the revival of hydrodynamic methodology.

After a brief description of the methodology in each case, practical tips and advice about the measurement and analysis will be provided—largely of the type not to be found in the manuals of commercial manufacturers. The interested reader can then find any other information needed from the latter and from the key references given.

2. Mass and quaternary structure measurement

It is worth stressing here that, unlike a polypeptide mass from sequence analysis or a protein structure from crystallography or NMR, a hydrodynamic mass or a conformation is a 'soft' quantity as opposed to a 'hard' one. That is to say, it will always come with a '±' and often with assumptions (about thermodynamic ideality, hydration, etc.). Although the molecular weight of an unglycosylated polypeptide can be determined to an accuracy of ± 1 Da from sequence information or from mass spectrometry (see Chapter 2), a similar precision cannot be obtained for glycosylated proteins because of polydispersity deriving from the variability of a cell's glycosylation process. Many proteins contain more than one non-covalently linked protein chain, particularly at higher concentrations. This can be uncovered by carrying out analyses under both native and denaturing conditions. An important role of hydrodynamic methods for mass analysis in protein chemistry is to give the molecular weight of the 'intact' or 'quaternary' structure and also to provide an idea of the strength of binding of these non-covalent entities through measurement of association constants.

2.1 Gel filtration and size exclusion chromatography

The simplest method of measuring molar mass is gel filtration (1), commonly referred to as 'gel permeation chromatography' or now 'size exclusion chromatography' (SEC), since the chemical inertness of the separation medium is assumed. Originally this was conceived as a method for the separation and purification of macromolecules, but has developed over the years in its 'calibrated' form as a very popular method for measuring protein molar masses both in native and dissociative conditions.

The separation medium is a cross-linked gel, traditionally cross-linked polysaccharide or polyacrylamide beads equilibrated with the appropriate buffer. The degree of cross-linking dictates the separation range of the gel: looser gels separate bigger molecules (see Chapter 1). Proper packing of columns requires some skill, and the user manuals as supplied by the commercial manufacturers are usually very comprehensive. The availability of HPLC versions makes the measurement particularly attractive for protein chemists.

Gel filtration or SEC depends on the principle that some of the space inside the gel particle is available to smaller molecules, but unavailable to larger molecules, which are excluded. Thus, when a solution is applied to a properly packed gel column (*Figure 1a*) only the dead space—between gel particles—is available to the excluded molecules, which therefore come off first when elution is commenced. The excluded molecules—the larger molecules—will thus have a smaller elution volume, V_e, and will elute first from the column (*Figure 1b*). Smaller macromolecules, having progressively

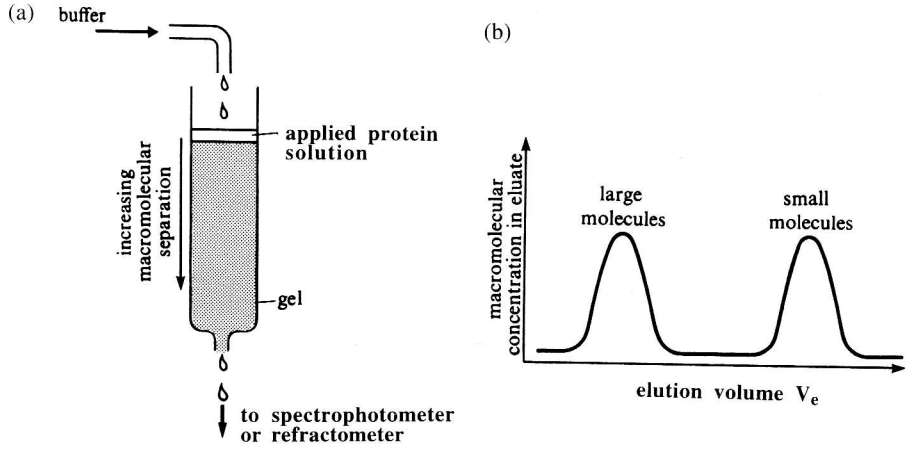

Figure 1. Principle of gel filtration and size exclusion chromatography. (a) Experimental set-up. (b) Example of an elution profile. Adapted from ref. 2.

more and more space available to them as molecular weight decreases, are accordingly eluted only at higher values of V_e. The separation is sometimes given in terms of the partition coefficient, K_{av}, defined by:

$$V_e = V_o + K_{av}(V_t - V_o) \quad [1]$$

where V_o and V_t are the 'void volume' and 'total volume' of the column, respectively. They are determined from separate elutions using solute species having partition coefficients of zero (totally excluded) and one (non-excluded), respectively. Elution of proteins as they emerge from the column is usually monitored spectrophotometrically. If the buffer contains absorbing reagents, like ATP, azide, etc., highly sensitive differential refractometers are now available, which are arguably preferable now as the detection method of choice.

All other things being equal, M_r and V_e are related empirically by the expression (1):

$$V_e = A - B \log_{10} M_r \quad [2]$$

where parameters A and B are properties of the column. This equation is valid only over the fractionation range of the gel; it also does not hold if other separation mechanisms are operating (4). To obtain M_r of a protein molecule or mixture of molecules, the column is first calibrated by the use of standard proteins of known size. Linear regression analysis is then used to evaluate A and B; hence M_r of the unknown protein can be found from its measured value of V_e. The calibration can only be applied within the fractionation range of the gel which depends on the pore size (*Figure 2*). Fractionation ability can be enhanced by running differing gel columns in

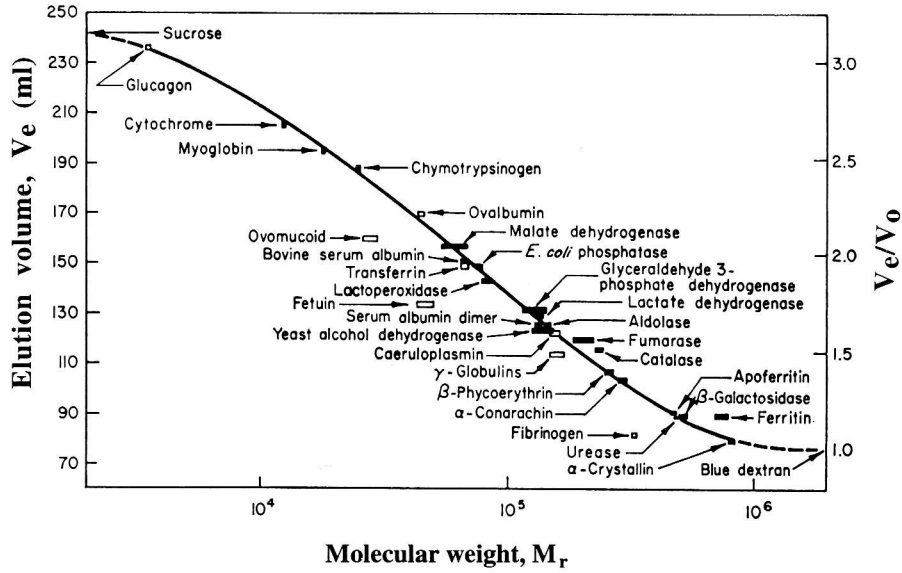

Figure 2. Calibration plot for proteins eluting from a Sephadex G200 column. From ref. 3.

series, a practice common with HPLC systems because of the much shorter elution times.

Equation 2 is valid only for molecules of similar shape and conformation. Thus calibration using globular protein standards would be inappropriate for fibrinogen and asymmetric muscle proteins like myosin and titin and for heavily glycosylated proteins. These calibration problems can be avoided by coupling an absolute molar mass detector (e.g. a light scattering photometer) downstream from the column (see Section 2.5).

The theory behind Equation 2 is not rigorous, but, at least for globular proteins, it seems to represent the data very well. For linear macromolecules of limited stiffness, there appears to be growing acceptance that the separation is more a logarithmic function of the hydrodynamic volume of a macromolecule ($\approx M_r[\eta]$ where $[\eta]$ is the intrinsic viscosity of a molecule) (see Section 3) and its corresponding hydrodynamic or 'effective' radius, r_H. This has culminated in a proposal for a 'universal calibration' (5). This may be more appropriate for proteins with disulfide bonds broken and in denaturing solvents, e.g. 6 M GdmCl. For such unfolded proteins, wider pore gels (such as Sepharose) are the most appropriate separation medium.

The procedure for gel filtration/ SEC analysis is given in *Protocol 1*.

2.2 Dynamic light scattering (DLS)

The appearance of simple to use fixed-angle (90°) dynamic light scattering photometers has made DLS an increasingly popular tool amongst protein

chemists. After certain assumptions and approximations, largely involving an assumed spherical shape, remarkably reliable estimates for the mol. wt of globular proteins have been obtained (6). When used in isolation, this method is, like gel filtration, a relative one, requiring calibration using standard proteins of known mol. wt. For asymmetric proteins like fibrinogen and myosin, the single angle approximation fails, but extraction of mol. wt and related parameters is still possible if a multi-angle instrument is used. Also, the primary parameter that comes from DLS measurements is the translational diffusion coefficient, D (in units of cm^2/sec), and it can be combined with results from sedimentation analysis in the analytical ultracentrifuge to determine M_r more accurately (see Equation 9 in Section 2.3.2).

Protocol 1. Estimating the size of a protein by low-pressure gel filtration/SEC

Equipment and reagents

- Column, with optional reservoir to assist packing
- Gel filtration matrix (e.g. Sephadex of the appropriate grade) equilibrated with buffer at temperature at which analysis is to be made
- Peristaltic pump
- Mol. wt calibration standards of similar shape and other conformational properties to the protein to be characterized

Method

1. Mount the empty column vertically, with the aid of a plumb-line. Attach outlet tubing and fill the column with buffer, removing all dead space. Close outlet.
2. Pack the column with the matrix; pour in a thick gel slurry (preferably degassed) in a single operation, avoiding air bubbles and keeping the temperature approximately constant.
3. Close off the the column without trapping any air; repeat with any additional columns that are to be used in series.
4. Attach peristaltic pump to the first column, and run through at least three column volumes of buffer to ensure equilibration (check tubing joints for leaks!). The maximum flow rate will depend upon the matrix (see manufacturers' specifications); typically, it is in the range 0.2–6 ml/min.
5. Attach a UV recorder downstream from the last column. To monitor most proteins, set the monitoring wavelength to 278 nm or, if the buffer is sufficiently transparent, to 210–230 nm, which will give greater sensitivity.
6. Measure the absorbance baseline of the buffer.
7. Inject samples of the mol. wt standards on to the column and measure their V_e.

Protocol 1. *Continued*

8. Calibrate the column by plotting V_e versus mol. wt for the standards.
9. Inject the test protein and measure its V_e under the same conditions.
10. Estimate the mol. wt of the test protein from its V_e and the calibration curve for the column.
11. Wash the column with three volumes of buffer.
12. If the column is to be used again at a later time, keep buffer flowing slowly through it; or include an anti-microbial agent, such as sodium azide, and store it in the cold.

2.2.1 Principle

The principle of DLS experiments is very simple (*Figure 3a*) and is based on the high intensity, monochromaticity, collimation, and coherence of laser light. Laser light is directed on to a thermostatted protein solution, and the intensity is recorded at either a single or multiple angles using a photomultiplier/photodetector. The intensities recorded will fluctuate with time caused by Brownian diffusive motions of the macromolecules; this movement causes a 'Doppler' type of wavelength broadening of the otherwise monochromatic light incident on the protein molecules. Interference between light at these wavelengths causes a 'beating' or fluctuation in intensity in much the same as a listener perceives a radio station with superposition of other radio stations at nearby frequencies. How rapid the intensity fluctuates (nsec to μsec time intervals) depends on the mobility or diffusivity of the protein molecules. A purpose-built computer, known as an autocorrelator, 'correlates' or interprets these fluctuations. It does this by evaluating a 'normalized intensity autocorrelation function'($g^{(2)}$) as a function of the 'delay time', τ (in the range of milli- to microseconds). The decay of the correlation, $g^{(2)}(\tau)$ as a function of τ, averaged over longer time intervals (usually minutes) can then be used, by an interfaced PC or equivalent, to obtain the value of D. Larger and/or asymmetric particles that move more sluggishly will have slower intensity fluctuations, slower decay of $g^{(2)}(\tau)$ with τ, and hence smaller D values compared to smaller and/or more globular particles. The delay time τ itself is the product of the 'channel number' b (taking on all integral values between 1 and 64, or up to 128 or 256 depending on how expensive the correlator) and a user-set 'sample time', τ_s; its value is typically ~ 100 nsec for a rapidly diffusing protein of low mol. wt (e.g. about 20 000) and increasing up to milliseconds for microbes. In the past, τ_s was selected by trial and error, but now modern data acquisition software usually does this automatically.

For spherical particles, a single term exponential describes the decay of Γ with τ:

$$g^{(2)}(\tau) - 1 = e^{-Dk^2\tau} \qquad [3]$$

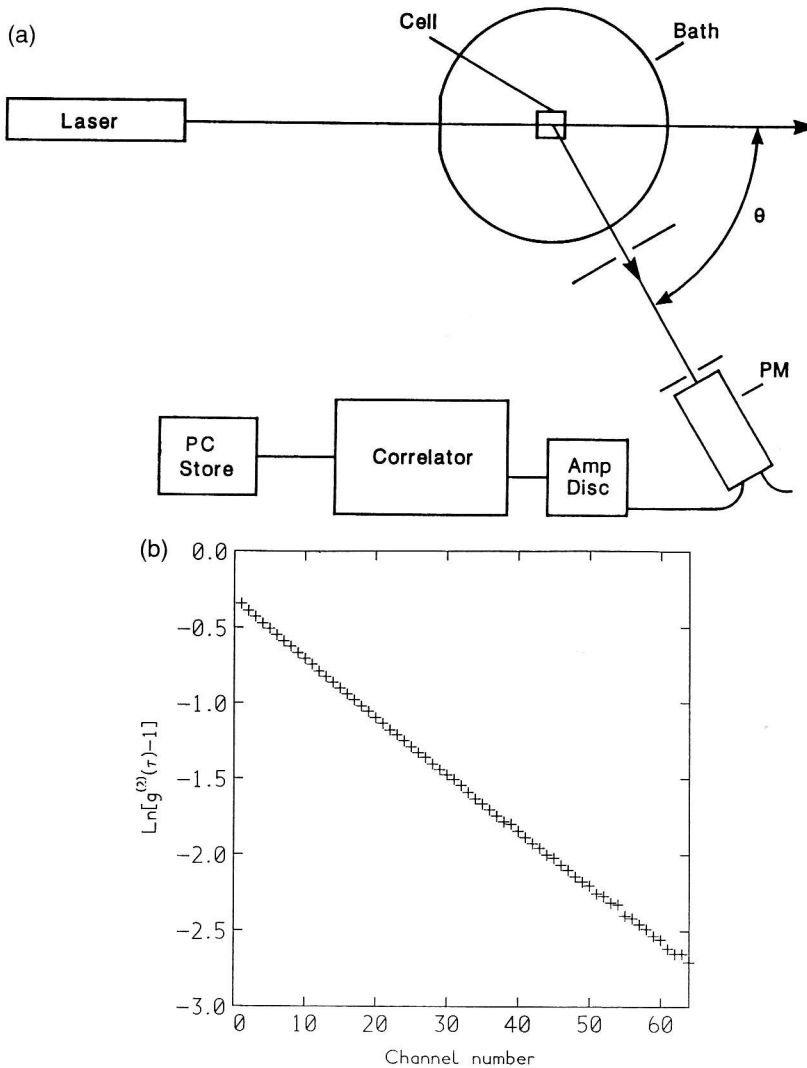

Figure 3. Principle of dynamic light scattering. (a) Experimental set-up. (b) Normalized autocorrelation decay plot for the protein assembly dynein (in 40 mM NaCl). $D^0_{20,w} = 1.1 \times 10^{-7}$ cm^2/sec; M_r (from Equation 9) $= 2.5 \times 10^6$. From ref. 7.

where k is the Bragg wave vector whose magnitude is defined by:

$$k = \{4\pi n/\lambda\} \sin(\theta/2) \qquad [4]$$

n is the refractive index of the medium, θ the scattering angle, and λ the wavelength of the incident light. Equation 3 can be reasonably applied to quasi-spherical particles like globular proteins or spheroidal protein assemblies (*Figure 3b*).

2.2.2 Fixed-angle (90°) DLS photometer

For globular proteins and spheroidal assemblies, application of Equation 3 at only a single fixed-angle is usually sufficient. Low angles are usually avoided because they magnify problems due to any contamination with dust or other supramolecular particles: an angle of 90° is normally used. For a given laser power at a given protein concentration, the smaller the protein the lower the intensity of scattered light, and hence the longer the averaging required to give a sufficient signal. A commercial instrument is available based on this single fixed-angle principle (6) (*Figure 4a*). Its operation is described in *Protocol 2.*

To obtain mol. wt information from the value of D, a calibration curve of log D versus log M_r is produced, based on globular protein standards and known as an 'MHKS' (Mark–Houwink–Kuhn–Sakurada) scaling relation (8) (*Figure 4b*). It is assumed that the same relation holds for the unknown protein.

Protocol 2. Measuring the diffusion coefficient and approximate molecular weight of a globular protein by fixed-angle DLS

Equipment

- Fixed-angle DLS photometer, such as the Protein Solutions 801 instrument
- Sterile syringe with appropriate filter, 0.1–0.45 μm, depending upon the size of the protein
- Deionized, distilled water
- Sample of protein in an appropriate buffer and close to the optimal concentration (for the Protein Solutions 801 instrument, 2 mg/ml for a 30 kDa protein, proportionally less for larger proteins)

Method

1. Inject water or buffer, via a 0.1 μm filter, into the warmed-up DLS photometer to obtain the clean water count rate.
2. Inject the sample in the same way, using the appropriate filter, and measure the count rate.
3. If the count rate is below the manufacturer's threshold, check the instrument alignment or increase the protein concentration.
4. Use the instrument's software to obtain the diffusion coefficient and, where appropriate, the in-built calibration to obtain directly the approximate mol. wt.
5. Rinse and dry the flow cell of the photometer.

Figure 4. Single-angle dynamic light scattering. (a) Photometer DynaPro 801 (courtesy of Protein Solutions Ltd.) incorporates a 20 mW infrared (780 nm) semiconductor laser. Photons scattered at an angle of 90° are collected by a lens and conducted to an avalanche photodiode via an optical fibre; this produces a single electrical pulse for each photon received and these are stored and correlated by an integral computer. The optical bench

(a)

(b)

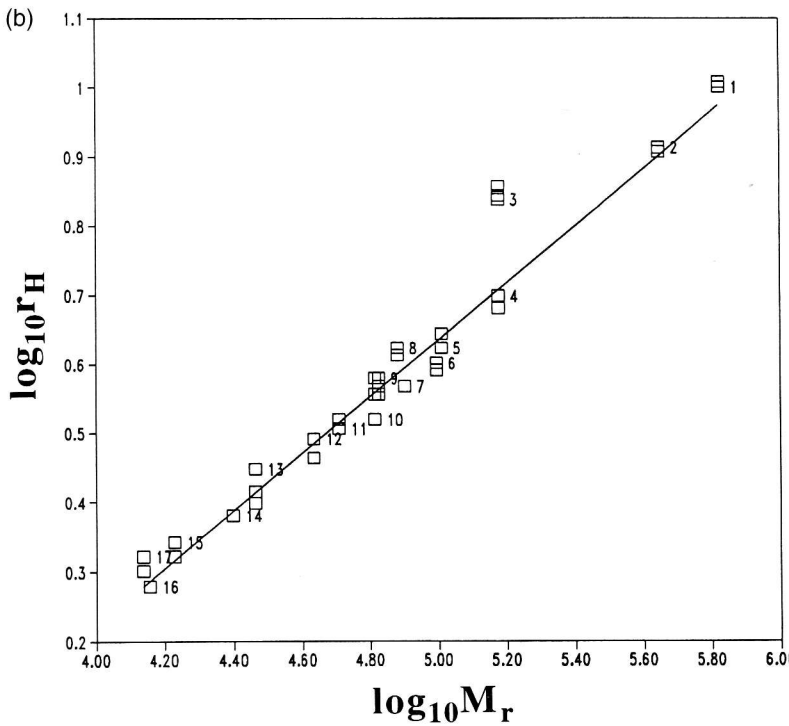

measures only 25 × 5 × 5 cm (6). (b) Double logarithmic calibration plot of r_H versus M_r for: 1, thyroglobulin; 2, apoferritin; 3, IgG; 4, yeast alcohol dehydrogenase; 5, hexokinase; 6, amyloglucosidase; 7, horse alcohol dehydrogenase; 8, transferrin; 9, bovine serum albumin; 10, haemoglobin; 11, hexokinase subunit; 12, ovalbumin; 13, carbonic anhydrase; 14, chymotrypsinogen; 15, myoglobin; 16, lysozyme; 17, ribonuclease A. From ref. 6.

Other approximations and practical requirements with the operation of this type of fixed-angle instrument have to be made:

(a) Solutions must be as free as possible from dust and supramolecular aggregates. This requirement is met by injection of the sample into the (scrupulously clean) scattering cell via a Millipore filter(s) of appropriate size (0.1–0.45 μm).

(b) The diffusion coefficient is a sensitive function of temperature and the viscosity of the solvent. The log D versus log M_r calibration must be made under the same temperature (kept constant during the measurement) and solvent viscosity conditions.

(c) The diffusion coefficient measured at a single concentration is an apparent one, D_{app}, because of non-ideality effects (finite volume and charge). These effects become vanishingly small as the concentration approaches zero. The approximation is made—usually reasonably for proteins—that $D_{app} \approx D$, or that any non-ideality effects are the same as for the calibration standards.

Despite these approximations, the values of diffusion coefficients and M_r obtained in this way have been remarkably reliable. For non-globular proteins, however, the log D versus log M_r calibration becomes invalid and Equation 3 no longer applies; resort has then to be made to an instrument with a multi-angle facility.

2.2.3 Multi-angle instruments

Measurements using multi-angle equipment (*Figure 5a*) are more time-consuming, and the instrumentation larger and more expensive. Data analysis is also more complicated. Equation 3 no longer applies, largely because of the added complication of rotational diffusion effects. These effects vanish, however, as the scattering angle θ approaches zero. It is therefore possible to use Equation 3 in terms of an apparent diffusion coefficient D_{app}, with contributions from both concentration and rotational diffusion effects. D_{app} is measured at several angles and extrapolated back to zero angle to give D if concentration effects are negligible. If, however, concentration dependence effects are suspected, a double extrapolation can be performed on the same plot (called a 'Dynamic Zimm plot') of D_{app} to zero angle and to zero concentration (10). The common intercept gives the 'ideal' (in a thermodynamic sense) diffusion coefficient, D^0. Because this quantity is not only an intrinsic property of the protein but also of the viscosity, η, and the temperature of the buffer, it has to be corrected to standard conditions (viscosity of pure water at 20°C, $\eta_{20,w}$), either before or after the extrapolation (11):

$$D^0_{20,w} = D^0 (\eta/\eta_{20,w}) (T/293.15). \quad [5]$$

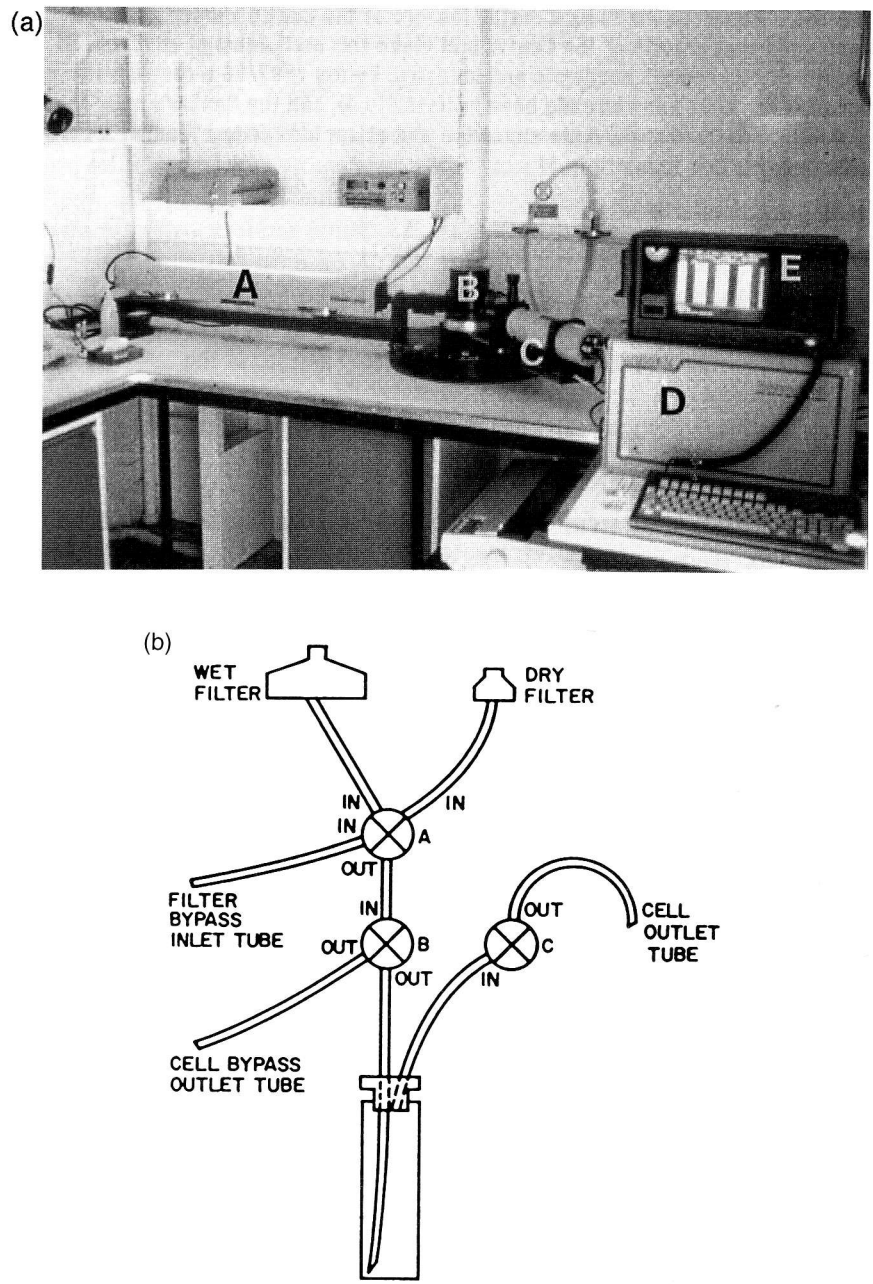

Figure 5. Multi-angle DLS. (a) Photometer Malvern Instruments 4700 system in our laboratory. A, 15 mW He-Ne laser; B, water-bath, goniometer; C, photomultipliers/amplifier discriminator; D, autocorrelator; E, PC. (b) Schematic of specially constructed cuvette designed to minimize the dust problem. From ref. 9.

The size of a protein, as represented by its equivalent hydrodynamic radius, r_H, is related to $D^0_{20,w}$ by the Stokes equation:

$$r_H = k_B T / (6\pi\eta_{20,w} D^0_{20,w}) \quad [6]$$

where k_B is Boltzmann's constant. To obtain an absolute measure of M_r of a protein from $D^0_{20,w}$, without assumptions concerning the shape of the protein, requires combination with the sedimentation coefficient from the analytical ultracentrifuge, as described in Section 2.3. Some modern software attempts to evaluate M_r directly from the diffusion coefficient; this should be treated with some caution.

2.2.4 Further notes

(a) For multi-angle measurements, preferences vary in terms of the type of cuvettes used. Square cuvettes are optically more reliable, but cell corners are obviously prohibited. Cylindrical cuvettes, if used, should be of the wide diameter type (> 2 cm) to avoid internal and stray reflections.

(b) Scrupulous attention to sample and cuvette clarity is mandatory, particularly for macromolecules of $M_r < 10^5$, which give low scattering signals, and if low angles are employed, where the effects of supramolecular contaminants are at their maximum. Special cuvette filling arrangements are used for clarification purposes (*Figure 5b*).

(c) The angular extrapolation of D_{app} can provide an estimate for the rotational diffusion coefficient, albeit to a lower precision than conventional methods (fluorescence depolarization, electric birefringence).

(d) If the protein is polydisperse or self-associating, the logarithmic plot of the type shown in *Figure 3b* will tend to be curved, and the corresponding diffusion coefficient will be a z-average (12). The spread of diffusion coefficients is indicated by a parameter known as the 'polydispersity factor' (12) which most software packages evaluate.

(e) Various computer packages are available from the commercial manufacturer for data acquisition and evaluation. In our laboratory, we prefer to acquire the data in ASCII format using the data capture software of the commercial manufacturer and then use our own in-house routine 'PROTEPS' (S. E. Harding, J. C. Horton, and P. Johnson, unpublished data) for the evaluation of diffusion coefficients and polydispersity factors.

(f) More advanced routines are available, such as 'CONTIN', designed for the study of heterogeneous systems by going beyond the use of polydispersity factors and inverting the autocorrelation data directly to give distributions of particle size. These methods have been recently reviewed (13).

(g) DLS is particularly valuable for the investigation of changes in macromolecular systems when the time-scale of changes is minutes or hours, and not seconds or shorter (14).

(h) For charged macromolecular systems, DLS provides a useful tool for monitoring electrophoretic mobilities (15), and commercial instrumentation is available for this purpose.

2.3 Sedimentation velocity in the analytical ultracentrifuge

Combination of the sedimentation coefficient, s, from sedimentation velocity with the diffusion coefficient, D, from DLS gives an absolute value for the mol. wt of a protein, without assumptions about conformation. This method for mol. wt measurement was given by T. Svedberg (16), the founder of the analytical ultracentrifuge: a technique which is now undergoing something of a renaissance with the launch of a new commercial instrument (*Figure 6a*) (17).

The basic principle of the technique is as follows: a solution of the protein is placed in a specially designed cell with sector-shaped channel and transparent end windows (*Figure 6b*). This in turn is placed in an appropriately balanced rotor and run in high vacuum at the appropriate speed (typically 50 000–60 000 r.p.m. for a protein of M_r 10^4 to 10^5, lower speeds for larger molecules). A light source positioned below the rotor transmits light via a monochromator or filter through the solution and a variety of optical components. The moving boundary is recorded at appropriate time intervals, either on photographic film, on chart paper, or as digital output fed directly into a PC. Measurement of the rate of the movement of the boundary (per unit centrifugal field) enables evaluation of the sedimentation coefficient. For an introduction, see ref. 11; for the state of the art, see two recent books (18,19).

2.3.1 Optical systems

Three principle optical systems can be employed:

- absorbance (in the range 200–700 nm)
- 'Schlieren' (refractive index gradient)
- Rayleigh interference

The simplest system is the absorbance system, and it is used in the Optima XL-A analytical ultracentrifuge available commercially, so it will be described here. Use of the other optical systems requires more specialist knowledge, and the interested protein chemist needs really to consult an expert.

Examples of sedimenting boundaries recorded using absorption optics are shown in *Figure 7*, using a highly purified preparation of an enzyme (*Figure 7a*) and a heterogeneous preparation of a DNA binding protein (Pf1) with a macromolecular component and a fast moving aggregate (*Figure 7b*). The procedure for obtaining such data is described in *Protocol 3*.

(a)

(b)

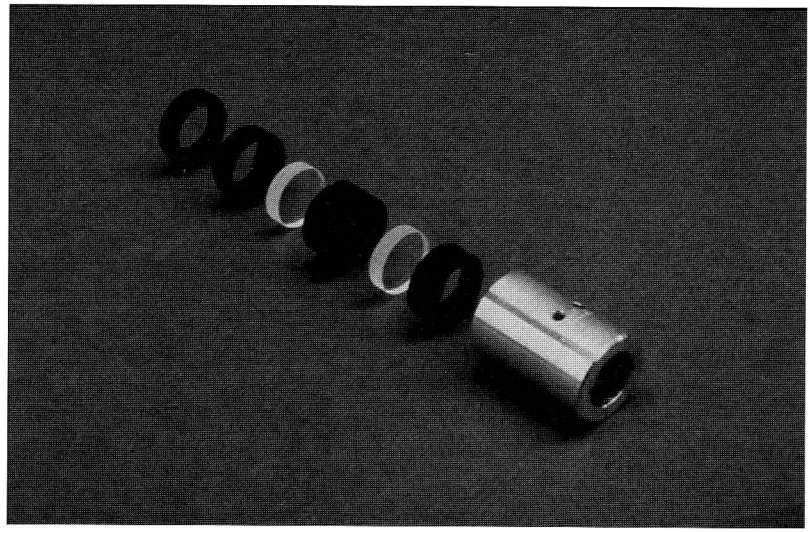

Figure 6. Modern analytical ultracentrifugation. (a) Beckman Optima XL-A in our laboratory, equipped with scanning absorption optics, with full on-line data capture and analysis. The rotor is stable down to ≈ 1000 rev. min, permitting the analysis of large macromolecular assemblies. (b) Components of an analytical cell (12 mm optical path length).

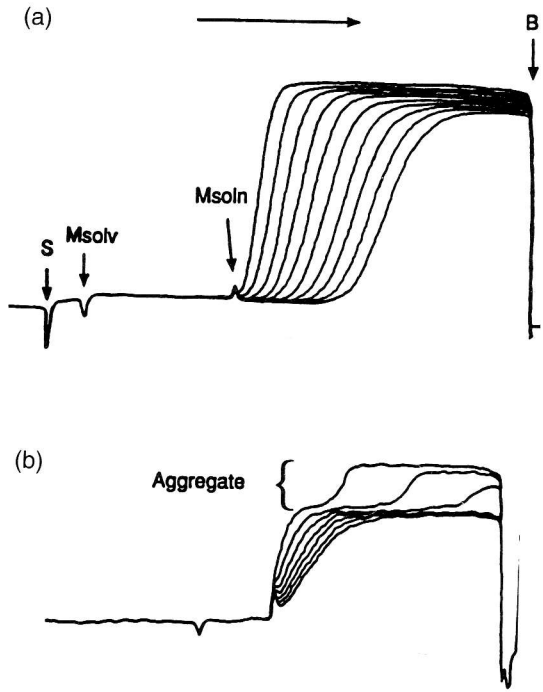

Figure 7. Sedimentation velocity diagrams obtained using scanning absorption optics. (a) Methylmalonyl mutase, 0.7 mg/ml. Monochromator wavelength 295 nm; scan interval 9 min; rotor speed 44 000 r.p.m.; temperature 20°C; measured s_{20} = (7.14 ± 0.04)S. (b) Gene 5 DNA-binding protein, 0.7 mg/ml. Monochromator wavelength, 278 nm; scan interval, 8 min; rotor speed, 40 000 r.p.m., temperature, 20°C; measured $s^0_{20,w}$ = (35.5 ± 1.4)S (faster boundary) and (2.6 ± 0.1)S (slower boundary).

Protocol 3. Sedimentation velocity measured with an analytical ultracentrifuge with scanning absorption optics detection system

Equipment

- Beckman Optima XL-A ultracentrifuge

Method

1. Concentration requirements for the protein. This depends on the extinction coefficient of the protein (see Chapter 10). The lower the protein concentration the better, since it minimizes problems of thermodynamic non-ideality. For proteins of average absorbance at 280 nm (≈ 500 ml/g/cm), concentrations as low as 0.2 mg/ml are possible with 12 mm optical path length cells. This can be made even

Protocol 3. *Continued*

lower if the buffer is transparent and the peptide bond wavelength can be used (210–230 nm). For absorbance values > 3, shorter path length cells need to be employed (the minimum is about 3 mm; below this, cell window problems become significant), 'off-maxima' wavelengths used (with caution), or, more desirably, a different optical system used (interference or Schlieren).

2. Choose the appropriate buffer/solvent. If possible, work with an aqueous solvent of sufficiently high ionic strength (> 0.05 M) to provide adequate suppression of non-ideality phenomena deriving from macromolecular charge effects (see below). If denaturing/dissociating solvents are used, appropriate centre-pieces need to be used (e.g. of the 'Kel-F' type; Beckman Instruments).
3. Load the sample into the cell. Double sector cells are used with the protein solution (0.2–0.4 ml) in one sector and the reference buffer or solvent in the other; the latter is filled to a slightly higher level to avoid complications caused by the signal coming from the solvent meniscus: the scanning system subtracts the absorbance of the reference buffer from that of the sample. Electronic multiplexing allows multiple hole rotors to be used, so that several samples can be run at a time.
4. Choose the appropriate temperature. The standard temperature at which sedimentation coefficients are quoted is now 20 °C (sometimes 25 °C). If the protein is thermally unstable (a sedimentation velocity run can take between one and a few hours), temperatures down to about 4 °C can be used without difficulty.
5. Choose the appropriate speed. For a small globular protein of sedimentation coefficient ~ 2 Svedbergs (S, where $1S = 10^{-13}$ sec), a rotor speed of 50 000 r.p.m. will give a measurable set of optical records after some hours. For larger protein systems (e.g. 12S globulins or 30S ribosomes), speeds of < 30 000 r.p.m. can be employed.
6. Measure the sedimentation coefficient, *s*. The sedimentation coefficient, *s*, is defined by the rate of movement of the boundary per unit centrifugal field: $s = (dr/dt)/\omega^2 r$, where r is the radial position of the boundary at time t, and ω is the angular velocity in radians/sec (ω = r.p.m. $\times 2\pi/60$). Commercial software is available for identifying the centre of the sedimenting boundary (strictly the '2nd moment' of the boundary is more appropriate; practically there is no real difference). Personal choices vary, but we find the most satisfactory method—if requiring a little more effort—is:
   (a) To plot out the boundaries (recorded at appropriate time intervals) using a high resolution printer or plotter and graphically draw a line through the user-identified boundary centres.

(b) Then use a graphics tablet to recapture the central boundary positions as a function of radial position.

Computer routines such as XLA-VEL (H. Cölfen and S. E. Harding, unpublished data) yield the sedimentation coefficient and a correction to the loading concentration for average radial dilution during the run (caused by the sector shape of the cell channels).

7. Correct the results to standard conditions. For each protein concentration used, correct the sedimentation coefficient, s, to standard conditions of buffer/solvent density and viscosity (water at 20°C, $\rho_{20,w}$ and $\eta_{20,w}$ respectively):

$$s_{20,w} = s\,(\eta/\eta_{20,w})\,\{(1 - \bar{\nu}\,\rho_{20,w})/(1 - \bar{\nu}\,\rho)\} \qquad [7]$$

where ρ is the density of the solvent. Knowledge of a parameter known as the 'partial specific volume', $\bar{\nu}$ (essentially the reciprocal of the anhydrous macromolecular density) is needed; this can usually be obtained for proteins from amino acid composition data, or measured with a precision density meter (20). Typically for proteins, $\bar{\nu}$ is close to 0.73 ml/g.

8. Extrapolate to zero protein concentration. Plot $s_{20,w}$ versus concentration (corrected for radial dilution) and extrapolate (usually linearly) to zero concentration (*Figure 8*) to give a parameter, $s^0_{20,w}$ which can be directly related to the frictional properties of the macromolecule (the so-called 'frictional ratio') and from which size and shape information can be inferred. If the protein is very asymmetric or solvated, plotting $1/s_{20,w}$ versus concentration generally gives a more useful extrapolation. The downward slope of a plot of $s_{20,w}$ versus concentration is a result of non-ideality behaviour and is characterized by the parameter k_s in the equation:

$$s_{20,w} = s^0_{20,w}\,(1 - k_s\,c). \qquad [8]$$

The value of k_s, which reflects non-ideality effects of the system, will depend on the size, shape, and charge of the protein. If the solvent used is of a sufficient ionic strength, charge effects can be suppressed.

2.3.2 Evaluation of molecular weight

The molecular weight, M_r, can be found by combination of $s^0_{20,w}$ with $D^0_{20,w}$ using the Svedberg equation:

$$M_r = (s^0_{20,w}/D^0_{20,w})\,\{R\,T/(1 - \bar{\nu}\,\rho_{20,w})\}. \qquad [9]$$

An accurate estimate for $\bar{\nu}$ as described above is normally required, since errors are tripled for proteins; e.g. an error of ± 1% in $\bar{\nu}$ results in an error of ± 3% in M_r. This means that care has to be made if the protein is glycosylated, since the $\bar{\nu}$ of carbohydrate is typically 0.6 ml/g.

For a heterogeneous system, $s^0_{20,w}$ will be a weight average and $D^0_{20,w}$ a

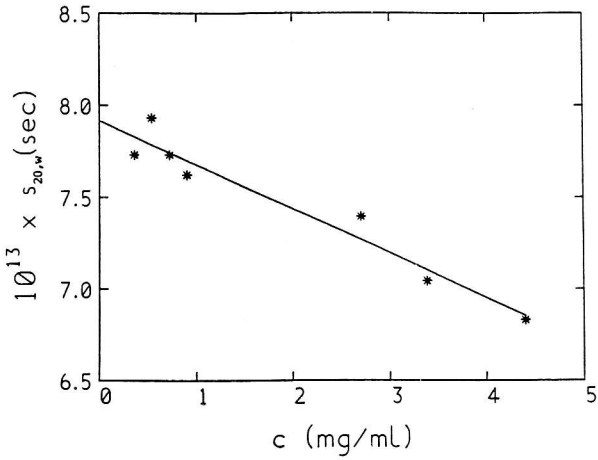

Figure 8. Sedimentation coefficient $s_{20,w}$ as a function of concentration for a rat IgE antibody. Measured $s^0_{20,w}$ = (7.92 ± 0.06)S.

z-average: the M_r calculated will also be a weight average (12), thus distinguishing it from the M_r obtained by osmometry (21), which is a number average.

A further approximate estimate can be obtained simply by combining $s^0_{20,w}$ with k_s (22):

$$M_r = (6\pi\,\eta_{20,w} s^0_{20,w})^{1.5}\,\{(3\bar{\nu})/4\pi).[(k_s/2\bar{\nu})-(\bar{\nu}_s/\bar{\nu})]\}^{0.5} \qquad [10]$$

where $\bar{\nu}_s$ is a specific volume allowing for hydration of the protein; since $(\bar{\nu}_s/\bar{\nu})$ in Equation 10 is usually small in comparison with $(k_s/2\bar{\nu})$, only an approximate estimate is needed. This method has given reliable estimates for standard protein molecules of known mol. wt. The parameter k_s is itself valuable for shape measurement. The form of the concentration-dependence can also be used as an assay for self-associating systems (23), although sedimentation equilibrium methods are usually superior (see Section 2.4).

2.3.3 Limitations

Sedimentation velocity is not so convenient for evaluating the molecular weights of proteins in denaturing/dissociating solvents, since their sedimentation coefficients are much smaller, due to greater frictional forces: s values of < 1S are difficult to measure with any precision because of the upper limit of rotor speed (60 000 r.p.m.). If these solvents are used, care has to be expressed concerning inertness of the cells used.

2.4 Sedimentation equilibrium

The 'sedimentation-diffusion' method for giving the mol. wt, although an absolute method, is rather inconvenient in that it requires two sets of measurements. A simpler method is to use one measurement by sedimentation

equilibrium, and it is probably the method of choice for mol. wt determination of intact protein assemblies, and for the investigation of interacting systems of proteins (24). The same instrument and optical system(s) for sedimentation velocity are used, the principal differences being:

- the much lower rotor speeds employed
- the longer run times
- the shorter solution (and buffer) columns in the ultracentrifuge cell; hence the smaller amount of material required

Sedimentation equilibrium, unlike sedimentation velocity, gel filtration, and dynamic light scattering, is not a transport method. In a sedimentation equilibrium experiment, the rotor speed is chosen to be sufficiently low so that the forces of sedimentation and diffusion on the macromolecular solute become comparable and an equilibrium distribution of solute is attained. This equilibrium can be established after a period of 2 to 96 hours, depending on the macromolecule, the solvent, and the run conditions. Since there is no net transport of solute at equilibrium, the recording and analysis of the final equilibrium distribution (*Figure 9*) will give an absolute estimate of the

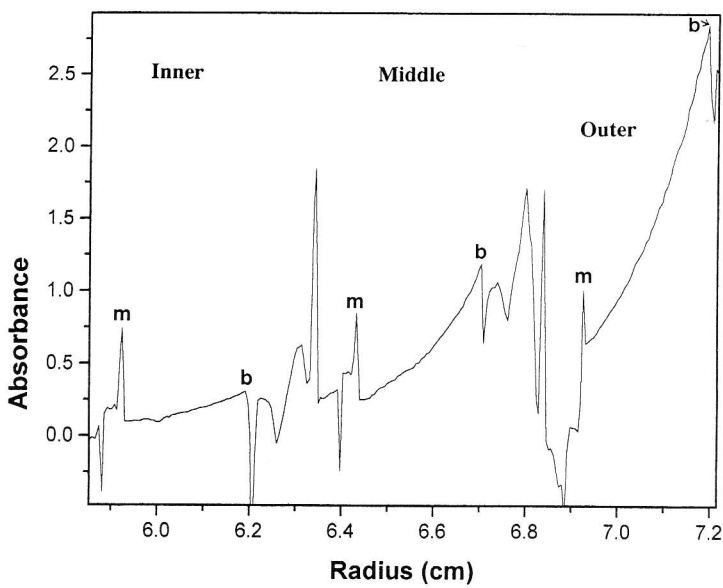

Figure 9. Sedimentation equilibrium profiles for β-lactoglobulin B. Absorption optics, with wavelength 280 nm. Rotor speed, 15 000 r.p.m.; temperature, 20°C. A multichannel cell (12 mm optical path length) was used allowing three solution/solvent pairs, with 0.12 ml in the solvent channels and 0.10 ml in the sample channels. The initial protein concentrations were 0.1 mg/ml (inner profile); 0.2 mg/ml (middle); 0.3 mg/ml (outer). Only absorbances < 1.5 could be used with the outer channel; this difficulty could have been overcome by using a longer wavelength. With the inner channel, the signal could have been increased by using a far-UV wavelength (210–230 nm).

protein mass and associated parameters, since frictional (i.e. shape) effects are not involved.

Protocol 4 refers only to the absorption system—because of its simplicity and availability—for recording the equilibrium distribution of solute in the ultracentrifuge cell. The most accurate method is, in fact, the interference system, but it requires considerable more expertise to operate correctly (11,18,19).

Protocol 4. Measuring the sedimentation/equilibrium profile of a protein

Equipment

- As in *Protocol 3*

Method

1. Choose the appropriate conditions. These are similar to those applying to sedimentation velocity (see *Protocol 3*). As with sedimentation velocity, a temperature of 4 °C can be used without difficulty. Sample volume requirements are lower than for sedimentation velocity: 0.1–0.2 ml gives a column length of about 0.1–0.2 mm with 12 mm cells. The longer the column, the greater the precision and the more information that can be extracted. The shorter the column, the quicker equilibrium will be reached (27), which may be important if many samples need to be run and/or the protein is relatively unstable.
2. Load the sample in the cell as in *Protocol 3.* As with sedimentation velocity, multiple cells can be run simultaneously in multihole rotors and electronically multiplexed. Further, because of the shorter columns needed for sedimentation equilibrium, special multichannel cells containing three sample/solvent pairs can be used (*Figure 9*). So, for a four-hole ultracentrifuge rotor (with one hole needed for the counterpoise with reference slits for calibrating radial positions in the cell), nine solutions can be run simultaneously. Eight-hole rotors are now available.
3. Choose the appropriate rotor speed.
4. Run the rotor until equilibrium is reached, when scans separated by sufficient time are identical. Smaller molecules get to equilibrium faster than larger ones. Less than 24 h are required for molecules of $M_r < 10^4$; large, slower diffusing molecules take 48–72 h. The time to equilibrium can be decreased by initial 'overspeeding', i.e. running at higher speed for a few hours before setting to the final equilibrium speed. It may, in some applications, be desirable to use shorter columns (as short as 0.5 mm); although the accuracy of the measure-

ments will be lower, this 'short column' method offers the advantage of reaching equilibrium in a few hours.

5. Record the equilibium profile. The parameter measured is the absorbance of the protein, A, as a function of the radial distance from the centre of the rotor, r. If scanning absorption optics are used, equilibrium patterns such as *Figure 9* can be read directly into an attached PC.

6. Measure the absorbance baseline. If the proteins are not too small, after the final equilibrium pattern has been recorded, the rotor is run for a short time at a higher speed (up to 60 000 r.p.m. or the upper limit for the particular centre-piece) to deplete the solution—or at least the meniscus region—of solute: the residual absorbance gives the baseline absorbance of the solvent. With small proteins, careful dialysis of the protein solution versus the reference solvent before the run may be necessary.

7. Calculate the molecular weight. The average slope of a plot of ln A versus r^2, (*Figure 10a*) will yield M_r:

$$M_r = (\mathrm{d}\ln A/\mathrm{d}r^2) \times 2RT/(1-\bar{v}\rho)\,\omega^2. \qquad [11]$$

As with Equation 9, an accurate estimate for the partial specific volume $\bar{v}$ is required; ρ is the density of the solvent.

8. Analyse for heterogeneity. For a non-associating, monodisperse system, the plot of ln A versus r^2 will be linear (*Figure 10b*); for a heterogeneous protein (containing interacting or non-interacting species of different molar mass), it will be curved upwards. This situation occurs with self-associating systems (see below) and with mixed solute or heavily glycosylated protein systems such as mucus glycoproteins. In this case the data can be treated in one of two ways:

   (a) An average slope is measured. This yields, as with Equation 9, the weight average mol. wt, M_w. For strongly curving plots or for systems where the cell baseline is not clearly defined, a procedure that uses a function known as M^* (25,26) is useful.

   (b) Local slopes (using a sliding strip procedure) (28) along the ln A versus r^2 curve can be obtained to give what is called 'point' weight average mol. wts, $M_w(r)$, as a function of either radial position (or the equivalent local concentration or absorbance). This procedure is particularly useful for the investigation of self-association phenomena and other types of heterogeneity; it also provides a method for extracting the z-average mol. wt, M_z:

$$M_z = \frac{\{M_w(r = \text{cell base}) - M_w(r = \text{meniscus})\}}{\{M_w(r = \text{cell base})A(\text{cell base}) - M_w(r = \text{meniscus})A(\text{meniscus})\}} \qquad [12]$$

   The ratio M_z/M_w can be used as an index of the heterogeneity of the sample and, for non-interacting systems, is a measure of the

Protocol 4. *Continued*

inherent polydispersity of a system; this is particularly relevant to the study of heavily glycosylated systems.

9. Examine whether any apparent heterogeneity in mol. wt is due to association of the protein. If the system is self-associating or involved in 'heterologous' association (i.e. complex formation), either the ln A versus r^2 plot or the $M_w(r)$ versus A plot can be used to measure the stoichiometry and strength of the interaction. There are several commercial software packages available,[a] and a recent article has reviewed three using the dimerizing β-lactoglobulin as a model system for self-associations (29). Methods are also available for distinguishing between self-associating and non-interacting mixtures.
10. Consider non-ideality. For larger macromolecules ($M_r \geq 10^5$), such as protein assemblies and heavily glycosylated systems and/or for more concentrated solutions, non-ideality (through macromolecular exclusion and any unsuppressed charge effects) may become significant, which will tend to cause downward curvature in the ln A versus r^2 plots. This can obscure heterogeneity phenomena, and the two effects (non-ideality and heterogeneity) can occasionally cancel to give a linear plot that can be misleading; this can be avoided by running at more than one initial protein concentration. If the sample is not significantly heterogeneous, a simple extrapolation from a single experiment of point (apparent) mol. wt to zero concentration (absorbance) can be made, to give the infinite dilution 'ideal' value (in general, reciprocals are usually plotted as in *Figure 11*) (30). Alternatively, several sedimentation equilibrium experiments performed at different initial concentrations and extrapolation of 'whole cell' molecular weights, $M_{w,app}$, to zero concentration are necessary.

[a] Software currently available from the commercial manufacturer tends to require an assumed model prior to the analysis (ideal monomer, self-association, non-ideal self-association, etc.). We find two other general packages, not requiring assumed models, of use. These are:

(a) MSTAR, written in-house (26) and now available for PC (H. Cölfen and S. E. Harding, unpublished data), which evaluates $M_{w,app}$ (using the M^* function), $M_{z,app}$, or $M_{w,app}$ (and also $M_{z,app}$, if the data are of sufficiently high quality) versus r or A.

(b) XLAse, which evaluates $M_{w,app}$ and $M_{z,app}$ (M. D. Lechner, Universität Osnabrück, unpublished data).

After these model-independent analyses have been performed, resort is then made to the more specialist packages (self-association, polydispersity, etc.). There exists now a highly useful e-mail system called RASMB for the exchange of software and other matters concerning analytical ultracentrifugation (RASMB database; W. F. Stafford, `stafford@edu.harvard.eri.bbri`).

2.5 Classical light scattering

This is another powerful absolute method for the determination of mol. wts of intact macromolecules, and it is particularly suited to the study of large

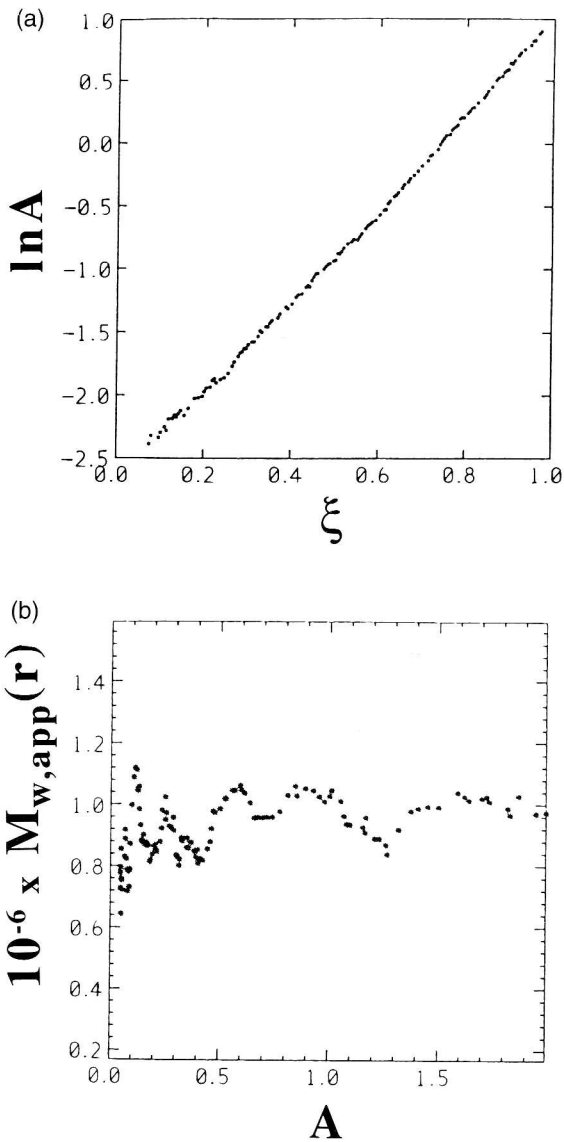

Figure 10. Sedimentation equilibrium data analysis for human IgM_1. Phosphate buffer pH 6.8; ionic strength, 0.1 M; protein concentration, ≈ 0.6 mg/ml. Scanning wavelength, 278 nm; rotor speed, 5000 r.p.m.; temperature, 20°C. (a) Log absorbance versus radial displacement squared plot. $\xi = (r^2 - a^2)(b^2 - a^2)$ where r is the radial displacement at a given point in the solute distribution and a and b the corresponding positions at the meniscus and cell base, respectively. From M^* analysis (25,26) of this data, $M_r = (1.00 \pm 0.02) \times 10^6$. (b) Plot of point average (apparent) M_r versus local concentration (expressed in absorbance units) in the solute distribution. Apart from noise near the meniscus there is no trend in the data, confirming a monodisperse, nearly ideal system. Adapted from ref. 26.

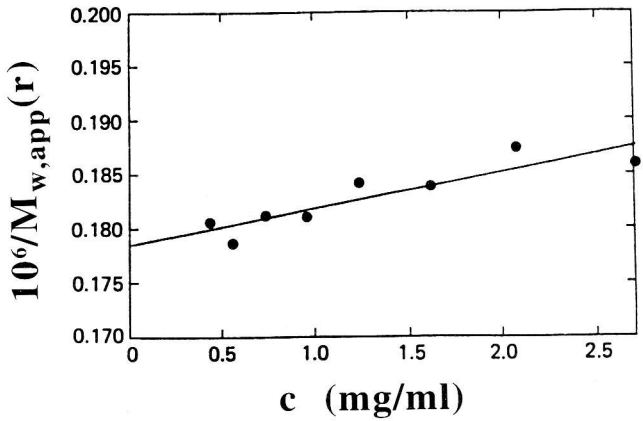

Figure 11. Plot of the reciprocal point (apparent) average molecular weight as a function of local concentration for turnip yellow mosaic virus. The measured M_r (from extrapolation to zero concentration) is $(5.8 \pm 0.2) \times 10^6$. Adapted from ref. 30.

macromolecular assemblies, up to a maximum of 50×10^6 M_r; beyond this the simple theory (known as the 'Rayleigh–Gans–Debye' approximation) breaks down. By 'classical' light scattering (as opposed to DLS) we mean the total or time-integrated intensity of light scattered by a macromolecular solution compared with the incident intensity for a range of concentrations and/or angles. Although a more rapid and, in principle, more convenient alternative to either the sedimentation-diffusion method or sedimentation equilibrium, the application of classical light scattering has until relatively recently suffered greatly from the 'dust problem', namely all solutions/scattering cells having to be scrupulously clear of dust and supramolecular particles, particularly for the analysis of proteins of mol. wt < 50 000; unlike for DLS, except for small proteins, measurements at low angles (where dust problems are their greatest) are mandatory. This has resulted in many cases in the requirement for unacceptably large amounts of purified material: experiments on incompletely purified solutions have been of little value.

Two developments have made the technique now worthy of serious consideration by protein scientists (31):

(a) The use of laser light sources, providing high collimation, intensity, and monochromaticity.

(b) The coupling of SEC-HPLC systems on-line to a light scattering photometer via the incorporation of a flow cell.

These facilitate considerably the analysis of mixtures of proteins and, more significantly, provide a very effective on-line 'clarification' system from dust and supramolecular contaminants. An example of such a set-up is given in *Figure 12*.

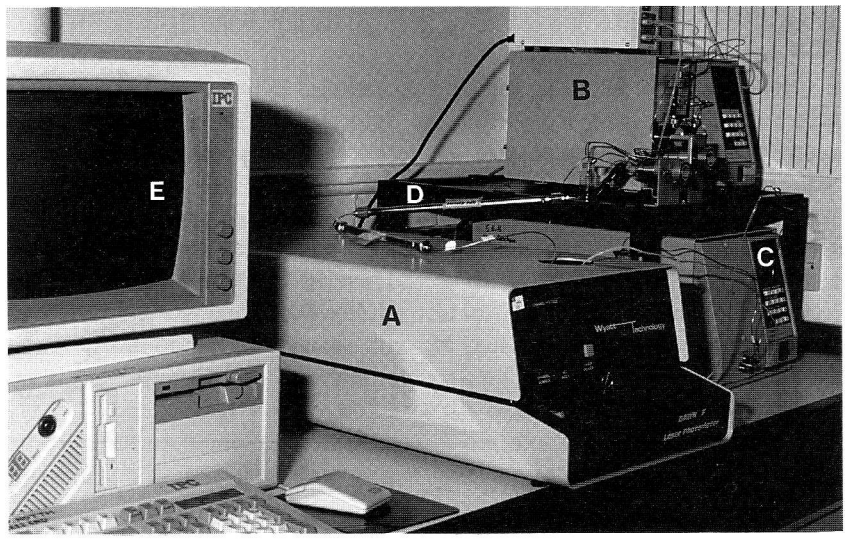

(b)

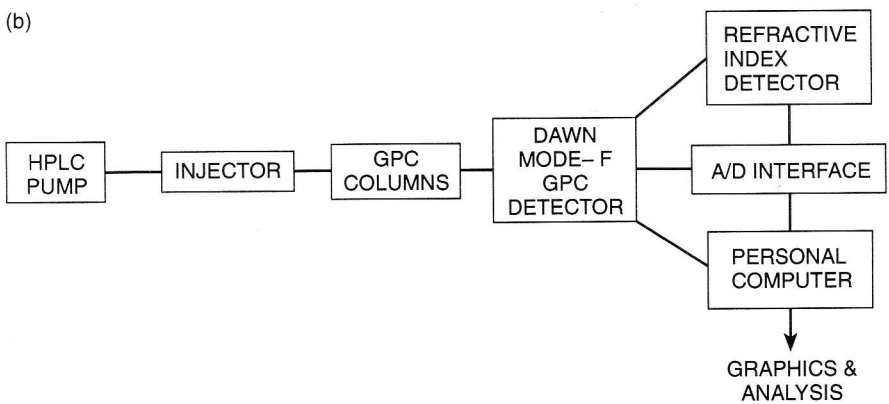

Figure 12. Multi-angle laser light scattering coupled to size exclusion chromatography (SEC-MALLS). (a) Experimental set-up in our laboratory. A, Dawn-F (Wyatt Technology); B, HPLC pump; C, refractive index detector; D, two SEC columns in series; E, interfaced PC system. (b) Schematic (courtesy of Wyatt Technology).

2.5.1 Principle

The intensity of light scattered by a protein solution is measured as a function of angle with a light scattering photometer (*Figure 12a*). For solutions of macromolecules or macromolecular assemblies, the basic equation for the angular dependence of light scattering is the Debye–Zimm relation:

$$Kc/R_\theta \approx \{1 + (16\pi^2 R_g^2/3\lambda^2) \sin^2[(\theta/2)]\}[(1/M_r) + 2Bc] \qquad [13]$$

where it is assumed that the second virial coefficient B (in units of ml mol g^{-2}) is sufficient to represent non-ideality (i.e. third and higher order terms are

assumed to be negligible); c is the protein concentration. R_θ is the Rayleigh excess ratio—the ratio of the intensity of excess light scattered (compared to pure solvent) at an angle θ to that of the incident light intensity (a $\cos\theta$ correction term is necessary if unpolarized light is used). K is an experimental constant dependent on the square of the buffer or solvent refractive index, the square of the refractive index increment (dn/dc in ml/g, analogous to the partial specific volume for proteins, and with a value of about 0.19 ml/g for proteins), and the inverse fourth power of the incident wavelength, λ. The parameter R_g is usually referred to as the 'radius of gyration' of the macromolecule, and is useful for conformation studies (see Section 3). If the macromolecular solute is heterogeneous, M_r will, as with sedimentation-diffusion and sedimentation equilibrium, be a weight average, M_w. Equation 13 is valid for particles of maximum dimension $< \lambda$ (i.e. $M_r < 50 \times 10^6$).

Normally, a double extrapolation to zero scattering angle and to zero protein concentration is necessary, using a procedure known as a Zimm plot (32). However:

(a) For particles of dimensions $< \lambda/20$ (i.e. $M_r < 50\,000$), the angular term in Equation 13 is small (i.e. $\sin^2(\theta/2) \approx 0$) and no angular dependence measurements are in principle necessary to obtain M_r (although this comes at a price: R_g cannot be measured if a conventional light source is used, although it can be measured using electromagnetic radiation of a lower wavelength—namely X-ray and neutron scattering (33)).

(b) More significantly, if the concentration is small enough (< 0.5 mg/ml for proteins and protein assemblies), the concentration term in Equation 13 is small (i.e. $Bc \approx 0$), and only an angular extrapolation is necessary. This is usually the situation with modern photometers designed with a flow cell for coupling on-line to an SEC system (31): after dilution through the column, the effective scattering concentration is usually ≤ 0.5 mg/ml. In these cases, Equation 13 becomes:

$$Kc/R_\theta \approx (1/M_r)\{1 + (16\pi^2 R_g^2/3\lambda^2) \sin^2[(\theta/2)]\} \qquad [14]$$

For the special case of globular proteins of $M_r < 50\,000$, the term Kc/R_θ is approximately equal to $1/M_r$ and no angular extrapolation is necessary. In this case, a large scattering angle (90°) is normally chosen, since at lower angles the greater noise/signal ratio is much more serious compared with the case for larger scatterers. To a further approximation:

$$R_\theta/Kc \approx M_r\{1-(16\pi^2 R_g^2/3\lambda^2) \sin^2[(\theta/2)]\}. \qquad [15]$$

2.5.2 SEC-MALLS

An example of a multi-angle laser light scattering photometer (MALLS) coupled to SEC is illustrated in *Figure 12*. The photometer is the DAWN-F system (Wyatt Technology). The angular scattering envelope is measured simultaneously by an array of photodiodes, unlike the moving photomulti-

plier system used by multi-angle dynamic light scattering photometers (*Figure 5a*). Equations 14 or 15 are used, or Equation 13 if the term Bc is significant and is known. From Equations 13–15, it is clear that it is necessary to have also a concentration detector, as well as the MALLS detector; this is normally a highly sensitive differential refractometer, also equipped with a flow cell (see corner of *Figure 12*).

For proteins, the principle value of this method is that it allows on-line clarification of the material from supramolecular aggregates. The method is, however, most valuable for the analysis of mixtures or for polydisperse heavily glycosylated protein systems such as mucus glycoproteins, since it provides weight-average masses and mass distributions without recourse to calibration standards required by SEC (Section 2.1). *Protocol 5* and *Figure 13* describe the various stages of analysis.

Protocol 5. SEC-MALLS analysis

Equipment

- SEC chromatography apparatus (see *Protocol 1*).[a] A pulse-free HPLC pump is essential. A guard filter upstream is desirable, as is pre-filtering solutions through an appropriate Millipore filter (e.g. 0.22 μm). For the Dawn-F system, a ≈ 100 μl microinjection loop is desirable. A column by-pass option can be installed if fractionation is not required (namely the Zimm plot or full application of Equation 13 is desired for a range of loading concentrations).
- Light scattering photometer, which must be calibrated (but not in a protein standards sense), usually with a strong Rayleigh (i.e. maximum dimension < λ/20) scatterer such as toluene, whose scattering properties are known (31). Calibration is necessary because the ratio of the intensities of the scattered and incident beams is usually very small (≈ 10^{-6}).[b]

Method

1. Determine accurately the delay in eluant volume or time between the light scattering photometer and the concentration (refractive index or UV absorbance) detector, so that the Kc/R_θ term in Equations 13–15 can be synchronized.
2. Record the SEC elution profile using the concentration detector (refractometer) and the light scattering. Only the 90° light scattering signal is shown in *Figure 13*.
3. Subject each elution volume V_e as it passes through the detectors to measurement of Kc/R_θ over the range of the angular scattering envelope. The resulting 'Debye plot' (Equation 15) yields the molar mass of each volume element.
4. Calibrate the column in terms of $\log_{10} M_r$ versus V_e.
5. Determine the weight-average molecular weights (and other derived averages such as the number and z-averages) and plot a relative mass distribution.
6. Determine the refractive increment, dn/dc (35). Its value is normally

Protocol 5. *Continued*

in the range of 0.18 to 1.19 ml/g for proteins, but can be as low as 0.15 ml/g for heavily glycosylated proteins.

[a] Choose SEC columns as appropriate. Molecules like the glycoprotein example of *Figure 13* are at the upper limit of resolution by gel columns. For larger particles, other methods of separation, on-line to the MALLS detector based on field flow fractionation are now available (36,37).

[b] For simultaneous multi-angle detection, the detectors have to be normalized to allow for the differing scattering volumes as a function of angle and the differing responses of the detectors. This is usually performed using a solution of a macromolecule of known M_r (generally $\leq$ 50 000) or for a solution of a larger macromolecule whose R_g is known (e.g. T-500 Dextran).

3. Shape measurement

Although the main thrust of this chapter has been on the estimation from hydrodynamic measurements of the molecular weight of a protein in its native state, the hydrodynamic parameters of a protein are also dependent upon the shape of the molecule. For mol. wt measurement, this can be a complication, although it can be overcome by combining the sedimentation and diffusion coefficients (Equation 9), each of which are affected similarly by the shape. Alternatively, transport methods can be avoided altogether by using either of the thermodynamic equilibrium-based techniques of sedimentation equilibrium and classical light scattering.

On the other hand, hydrodynamic methods provide information about the macromolecular shape. There is the complication that the hydrodynamic shape parameters obtained also depend upon the extent of hydration of the protein (i.e. the amount of aqueous solvent chemically bound or physically entrapped), which is very difficult to measure with any real precision. A further problem is that the more complicated the shape model used, the greater the number of independent parameters needed to specify the model uniquely. For example, to specify uniquely the radius of a spherical model requires only one parameter; for the axial ratio of an ellipsoid of revolution (i.e. an ellipsoid with two equal axes), two parameters are needed; for a general triaxial ellipsoid, with three unequal axes, three parameters are needed (38). All of these approaches are known as 'whole-body' approaches. The most complex way of representing shape is 'hydrodynamic bead modelling', where the protein structure is approximated as an array of spherical beads (39). Problems of the uniqueness of any such model are considerable, however, and this form of modelling is best used for choosing between plausible structures (e.g. subunit arrangements in a multisubunit protein, such as the angle between the two Fab arms of an antibody molecule) or for refining a crystallographic or NMR structure to dilute solution conditions. Segmental flexibility can also, in principle, be modelled using this latter approach.

The choice of hydrodynamic shape parameters is wide:

(a) The 'Perrin' frictional ratio (from the sedimentation or diffusion coefficients).

(b) The various rotational frictional ratios or relaxation times (from fluorescence depolarization or electro-optic measurements).

(c) The viscosity increment (from measurement of the intrinsic viscosity).

(d) The concentration-dependence of the sedimentation coefficient.

(e) The radius of gyration from solution X-ray scattering (or for proteins of $M_r > 50000$, from classical light scattering).

(f) The molecular co-volume of the protein (from measurements of the non-ideality parameter B in osmotic pressure, sedimentation equilibrium, or classical light scattering measurements).

The viscosity and rotational friction parameters are among the more sensitive but can be correspondingly more difficult to measure. The hydration problem is most effectively dealt with by combining two parameters to give 'hydration-independent' shape parameters.

Whereas the extraction of mol. wt information is relatively straightforward, the extraction of shape information is generally not, and the details are outside the scope of this chapter. The interested reader is referred to a recent article that examines in detail the various approaches and provides the necessary references (8). Suffice here to mention some PC software algorithms for hydrodynamic conformation analysis using either the simpler 'whole-body' or the 'hydrodynamic bead' algorithms.

3.1 Computer programs for conformational analysis

For ellipsoid modelling, we have in-house a suite of algorithms that have been transferred from mainframe FORTRAN to PC (BASIC and FORTRAN). ELLIPS1 (40) evaluates the axial ratio for prolate and oblate ellipsoids for a user-specified value of a hydrodynamic parameter. It is based on polynomial approximations to the full hydrodynamic equations, but the accuracy of this approximation is normally well within the precision of the measurement. ELLIPS2 uses the full hydrodynamic equations for general triaxial ellipsoids to specify the set of hydrodynamic parameters for any given value of the axial ratios. ELLIPS3 and ELLIPS4 carry out the reverse procedure, using a variety of graphical combinations of hydration-independent triaxial shape functions. Elsewhere, the routines HYDRO and SOLPRO developed by J. Garcia de la Torre and colleagues (41,42) are particularly useful for the application of bead models; to facilitate its application, a front-end algorithm (A to B) has been constructed to enable TRV to predict the set of hydrodynamic parameters for a given set of crystal structure co-ordinates (O. Byron, PhD dissertation, 1992, University of Nottingham, UK).

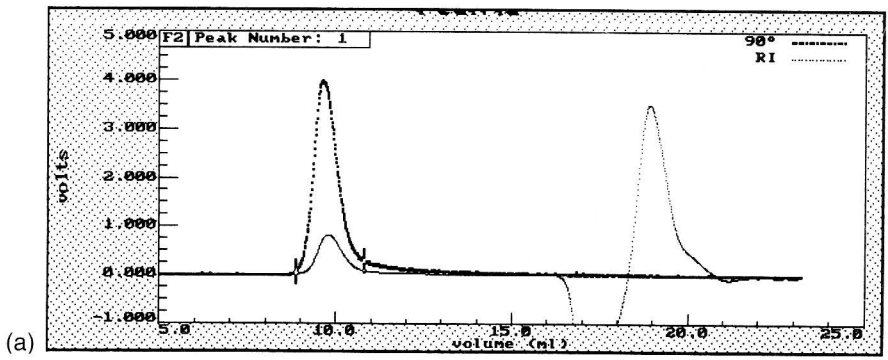
F2 Peak Number: 1
90°
RI
volts
5.000
4.000
3.000
2.000
1.000
0.000
-1.000
5.0
10.0
15.0
20.0
25.0
volume (ml)

(a)

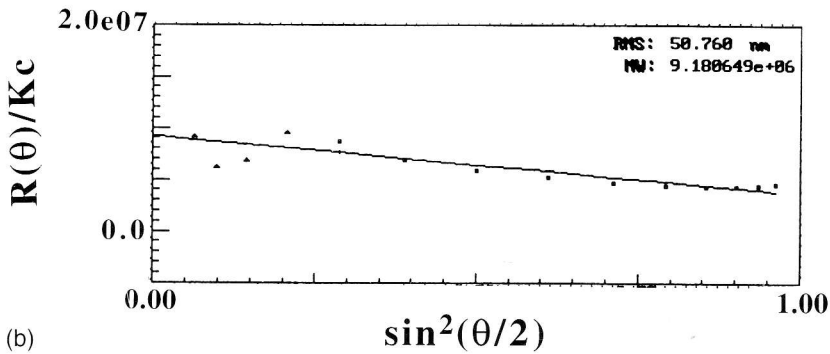
2.0e07
R(θ)/Kc
0.0
0.00
1.00
sin²(θ/2)
RMS: 50.760
MW: 9.180649e+06

(b)

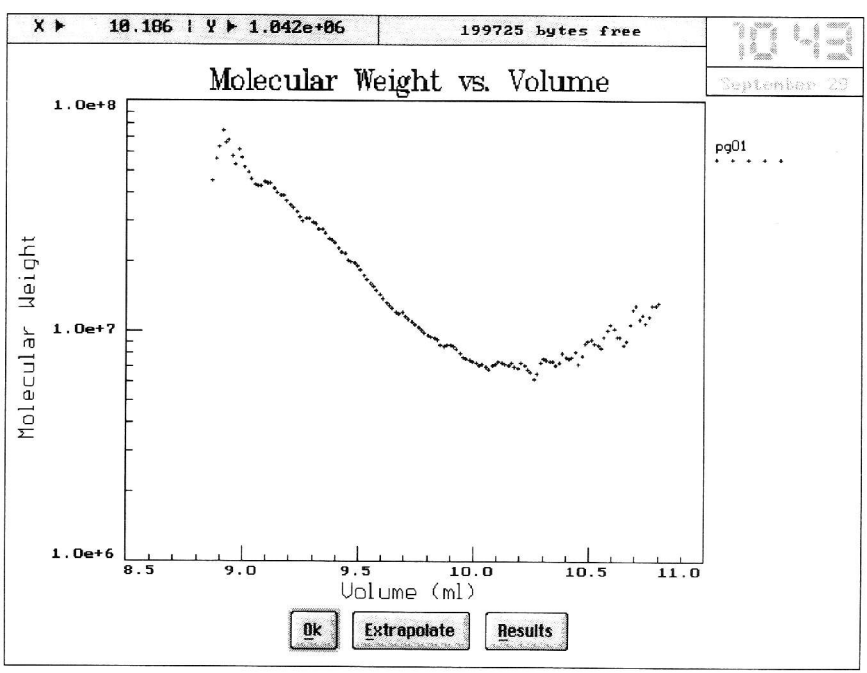
X ▶ 10.186 | Y ▶ 1.042e+06
199725 bytes free
Molecular Weight vs. Volume
pg01
1.0e+8
1.0e+7
1.0e+6
Molecular Weight
8.5
9.0
9.5
10.0
10.5
11.0
Volume (ml)
Ok
Extrapolate
Results

(c)

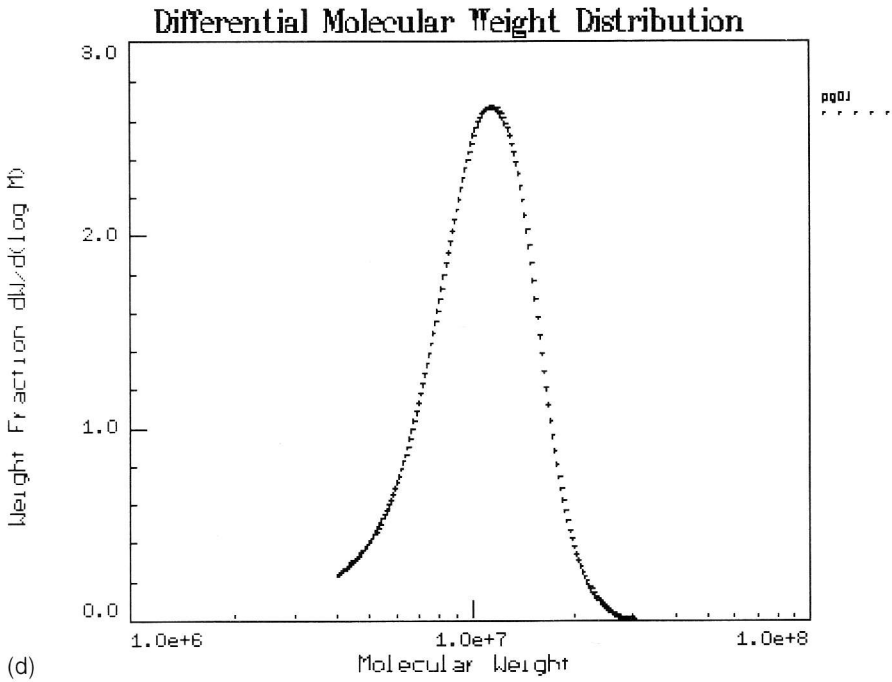

Figure 13. Extraction of mol. wt distribution of a high mol. wt glycoprotein (a pig gastric mucin preparation '5B1') using SEC-MALLS. (a) Elution profile recorded using the concentration (refractive index) detector (lower profile, lighter dots) and the MALLS detector (only 90° detection shown). The negative and positive peaks at high elution volume correspond to salt elution. (b) 'Debye' plot for a specific value of V_e. (c) Absolute logarithmic calibration plot showing clearly the 'range'of the gel. (d) Mol. wt distribution. The commercial manufacturers software was used for all the analyses: (a–c) ASTRA, (d) EASI. From ref. 34.

References

1. Ackers, G. (1975). In *The proteins* (3rd edn) (ed. H. Neurath and R. L. Hill), Vol. 1, p. 1. Academic Press, New York.
2. Furth, A. and Moore, R. (1986). *Self assembly of macromolecules*, p. 57. Open University Press, Milton Keynes, UK.
3. Andrews, P. (1965). *Biochem. J.*, **91**, 22.
4. Barth, H. G. (1980). *J. Chromatogr. Sci.*, **18**, 409.
5. Dubin, P. L. and Principi, J. M. (1989). *Div. Polym. Chem. Am. Chem. Soc. Preprints*, **30**, 400.
6. Claes, P., Dunford, M., Kennedy, A., and Vardy, P. (1992). In *Laser light scattering in biochemistry* (ed. S. E. Harding, D. B. Sattelle, and V. A. Bloomfield), p. 66. Royal Society of Chemistry, Cambridge, UK.
7. Wells, C., Molina-Garcia, A. D., Harding, S. E., and Rowe, A. J. (1990). *J. Muscle Res. Cell Motil.*, **11**, 344.

8. Harding, S. E. (1995). *Biophys. Chem.*, **55**, 69.
9. Sanders, A. H. and Cannell, D. S. (1980). In *Light scattering in liquids and macromolecular solutions* (ed. V. Degiorgio, M. Corti, and M. Giglio), p. 173. Plenum, New York.
10. Burchard, W. (1992). In *Laser light scattering in biochemistry* (ed. S. E. Harding, D. B. Sattelle, and V. A. Bloomfield), p. 3. Royal Society of Chemistry, Cambridge, UK.
11. Van Holde, K. E. (1985). *Physical biochemistry* (2nd edn), p. 110. Prentice Hall, Englewood Cliffs, New Jersey.
12. Pusey, P. N. (1974). In *Photon correlation and light beating spectroscopy* (ed. H. Z. Cummins and E. R. Pike), p. 387. Plenum, New York.
13. Johnsen, R. M. and Brown, W. (1992). In *Laser light scattering in biochemistry* (ed. S. E. Harding, D. B. Sattelle, and V. A. Bloomfield), p. 77. Royal Society of Chemistry, Cambridge, UK.
14. Harding, S. E. (1986). *Biotech. Appl. Biochem.*, **8**, 489.
15. Langley, K. H. (1992). In *Laser light scattering in biochemistry* (ed. S. E. Harding, D. B. Sattelle, and V. A. Bloomfield), p. 151. Royal Society of Chemistry, Cambridge, UK.
16. Svedberg, T. and Pedersen, K. O. (1940). *The ultracentrifuge*. Oxford University Press.
17. Giebler, R. (1992). In *Analytical ultracentrifugation in biochemistry and polymer science* (ed. S. E. Harding, A. J. Rowe, and J. C. Horton), p. 16. Royal Society of Chemistry, Cambridge, UK.
18. Harding, S. E., Rowe, A. J., and Horton, J. C. (ed.) (1992). *Analytical ultracentrifugation in biochemistry and polymer science*. Royal Society of Chemistry, Cambridge, UK.
19. Schuster, T. M. and Laue, T. M. (1994). *Modern analytical ultracentrifugation*. Birkhäuser, Boston.
20. Kratky, O., Leopold, H., and Stabinger, H. (1973). In *Methods in enzymology* (ed. C. H. W. Hirs and S. N. Timasheff), Vol. 27D, p. 98. Academic Press, New York.
21. Tombs, M. P. and Peacocke, A. R. (1974). *The osmotic pressure of biological macromolecules*. Oxford University Press, Oxford.
22. Rowe, A. J. (1992). In *Analytical ultracentrifugation in biochemistry and polymer science* (ed. S. E. Harding, A. J. Rowe, and J. C. Horton), p. 394. Royal Society of Chemistry, Cambridge, UK.
23. Gilbert, L. M. and Gilbert, G. A. (1973). In *Methods in enzymology* (ed. C. H. W. Hirs and S. N. Timasheff), Vol. 27, p. 273. Academic Press, New York.
24. Schachman, H. K. (1989). *Nature*, **341**, 259.
25. Creeth, J. M. and Harding, S. E. (1982). *J. Biochem. Biophys. Methods*, **7**, 25.
26. Harding, S. E., Horton, J. C., and Morgan, P. J. (1992). In *Analytical ultracentrifugation in biochemistry and polymer science* (ed. S. E. Harding, A. J. Rowe, and J. C. Horton), p. 275. Royal Society of Chemistry, Cambridge, UK.
27. Correia, J. J. and Yphantis, D. A. (1992). In *Analytical ultracentrifugation in biochemistry and polymer science* (ed. S. E. Harding, A. J. Rowe, and J. C. Horton), p. 231. Royal Society of Chemistry, Cambridge, UK.
28. Teller, D. C. (1973). In *Methods in enzymology* (ed. C. H. W. Hirs and S. N. Timasheff), Vol. 27D, p. 346. Academic Press, New York.
29. Joss, L. A. and Ralston, D. B. (1995). *Anal Biochem.*, in press.

30. Harding, S. E. and Johnson, P. (1985). *Biochem. J.*, **231**, 549.
31. Wyatt, P. J. (1992). In *Laser light scattering in biochemistry* (ed. S. E. Harding, D. B. Sattelle, and V. A. Bloomfield), p. 35. Royal Society of Chemistry, Cambridge, UK.
32. Tanford, C. (1961). *Physical chemistry of macromolecules*. J. Wiley & Sons, New York.
33. Perkins, S. J. (1994). In *Microscopy, optical spectroscopy and macroscopic techniques* (ed. C. Jones, B. Mulloy, and A. H. Thomas), p. 39. Humana Press, New Jersey.
34. Jumel, K., Fiebrig, I., and Harding, S.E. (1995). *Int. J. Biol. Macromol.*, **18**, 133.
35. Huglin, M. B. (ed.) (1972). *Light scattering from polymer solutions*. Academic Press, New York.
36. Arner, E. C. and Kirkland, J. J. (1992). In *Analytical ultracentrifugation in biochemistry and polymer science* (ed. S. E. Harding, A. J. Rowe, and J. C. Horton), p. 209. Royal Society of Chemistry, Cambridge, UK.
37. Adophi, U. and Kulicke, W. M. (1996). *Polymer*, in press.
38. Harding, S. E. (1989). In *Dynamic properties of biomolecular assemblies* (ed. S. E. Harding and A. J. Rowe), p. 32. Royal Society of Chemistry, Cambridge, UK.
39. Garcia de la Torre, J. (1989). In *Dynamic properties of biomolecular assemblies* (ed. S. E. Harding and A. J. Rowe), p. 3. Royal Society of Chemistry, Cambridge, UK.
40. Harding, S. E., Horton, J. C., and Cölfen, H. (1996). *Eur. Biophys. J.*, in press.
41. Garcia de la Torre, J., Navarro, S., Lopez-Martinez, M. C., Diaz, F. G., and Lopez-Cascoles, J. J. (1994). *Biophys. J.*, **67**, 530.
42. Garcia de la Torre, J., Carrasco, B., and Harding, S. E. (1996). *Eur. Biophys. J.*, in press.